An amplitude analysis of the process $e^+e^- \to 4\pi$ in the center-of-mass energy range 900–2000 MeV with the CMD-3 detector at the VEPP-2000 e^+e^- collider

E. A. Kozyrev[1,2], R. R. Akhmetshin[1,2], A. N. Amirkhanov[1,2], A. V. Anisenkov[1,2], V. M. Aulchenko[1,2], V. Sh. Banzarov[1], N. S. Bashtovoy[1], D. E. Berkaev[1,2], A. E. Bondar[1,2], A. V. Bragin[1], S. I. Eidelman[1,2,5], D. A. Epifanov[1,2], L. B. Epshteyn[1,2,3], A. L. Erofeev[1,2], G. V. Fedotovich[1,2], S. E. Gayazov[1,2], A. A. Grebenuk[1,2], S. S. Gribanov[1,2], D. N. Grigoriev[1,2,3], F. V. Ignatov[1,2], V. L. Ivanov[1,2], S. V. Karpov[1], V. F. Kazanin[1,2], I. A. Koop[1,2], A. N. Kirpotin[1], A. A. Korobov[1,2], A. N. Kozyrev[1,3], P. P. Krokovny[1,2], A. E. Kuzmenko[1,2], A. S. Kuzmin[1,2], I. B. Logashenko[1,2], P. A. Lukin[1,2], K. Yu. Mikhailov[1], V. S. Okhapkin[1], Yu. N. Pestov[1], A. S. Popov[1,2], G. P. Razuvaev[1,2], Yu. A. Rogovsky[1], A. A. Ruban[1], N. M. Ryskulov[1], A. E. Ryzhenenkov[1,2], A. V. Semenov[1,2], Yu. M. Shatunov[1], P. Yu. Shatunov[1,2], V. E. Shebalin[1,2], D. N. Shemyakin[1,2], B. A. Shwartz[1,2], D. B. Shwartz[1,2], A. L. Sibidanov[1,4], E. P. Solodov[1,2], V. M. Titov[1], A. A. Talyshev[1,2], A. I. Vorobiov[1], I. M. Zemlyansky[1], and Yu. V. Yudin[1,2]

[1]Budker Institute of Nuclear Physics, SB RAS, Novosibirsk, 630090, Russia
[2]Novosibirsk State University, Novosibirsk, 630090, Russia
[3]Novosibirsk State Technical University, Novosibirsk, 630092, Russia
[4]University of Victoria, Victoria, BC, Canada V8W 3P6
[5]Lebedev Physical Institute RAS, Moscow, 119333, Russia

Abstract. A large data sample of $e^+e^- \to 4\pi$ collected by the CMD-3 experiment at the VEPP-2000 e^+e^- collider allowed for an amplitude analysis of the process $e^+e^- \to 4\pi$ in the center-of-mass energy range 900–2000 MeV. Various intermediate components were distinguished and dominance of the $\omega\pi^0$ and $a_1\pi$ amplitudes has been proved.

1 Introduction

The study presented in the paper is aimed to shed light on the intermediate dynamics of the process $e^+e^- \to 4\pi$, i.e., to probe the structure of the hadronic current of the reaction in the energy range $E_{c.m.} = 0.9$–2.007 GeV. There is rich intermediate dynamics in the process and amplitude analysis can be useful in understanding how non-perturbative QCD proceeds. In addition, the process $e^+e^- \to 4\pi$ dominates in the energy region between 1 and 2 GeV and gives the largest part of the hadronic vacuum polarization uncertainty. Thus, its precise measurement will strongly affect precise tests of SM, e.g., g-2 interpretation.

Previously, amplitude analysis of $e^+e^- \to 4\pi$ was performed by the CMD-2, BaBar and CLEO collaborations. BaBar [1, 2]carried out the most precise cross section measurement in the region $E_{c.m.} = 0.85 \div 4.5$ GeV, but analysis of the intermediate amplitudes was not complete, though simple calculations based on selection cuts of the $\omega\pi^0$, $\rho f_0(980), \rho^+\rho^-$ states were made. Some evidence for the presence of the ρf_2 state was also obtained at $E_{c.m.} >$

1.8 GeV. The CMD-2 collaboration also published the results of the amplitude analysis in the energy range $1.05 < E_{c.m.} < 1.38$ GeV based on 22k events [3]. The dominance of the $\omega\pi^0$ and $a_1\pi$ was observed and other intermediate states were not found. Another analysis performed by CLEO [4] using about 24.5k events of the decay $\tau \to \pi^- 3\pi^0 \nu_\tau$ considered additional amplitudes. This analysis found that the models, providing the best description of the data, are dominated by $\omega\pi^0$ and $a_1\pi$ with small additional contributions of the $\sigma\rho$, $f_0(980)\rho$ or non-resonant $\rho\pi\pi$ channels.

2 CMD-3 detector and data set

The Cryogenic Magnetic Detector (CMD-3) described elsewhere [5] is installed in one of the two interaction regions of the VEPP-2000 e^+e^- collider [6]. The detector tracking system consists of the cylindrical drift chamber (DC) and double-layer cylindrical multiwire proportional Z-chamber, both installed inside a thin (0.085 X_0) superconducting solenoid with 1.3 T magnetic field. DC contains 1218 hexagonal cells and provides a measurement of charged particle momentum and of the polar (θ) and azimuthal (ϕ) angles. An amplitude information from the DC wires is used to measure the ionization losses dE/dx of charged particles with $\sigma_{dE/dx} \approx$ 11-14% accuracy for minimum ionization particles. A barrel electromagnetic calorimeter placed outside the solenoid consists of two subsystems: an inner liquid xenon (LXe) calorimeter (5.4 X_0 thick) surrounded by a scintillation CsI crystal calorimeter (8.1 X_0 thick) [7]. BGO crystals with 13.4 X_0 are used as an endcap calorimeter. The detector has two triggers: neutral and charged. A signal for the neutral one is generated by the information from the calorimeters, while the charged trigger comes from the tracking system. The return yoke of the detector is surrounded by scintillation counters which veto cosmic events.

To obtain a detection efficiency, Monte Carlo (MC) simulation of the detector based on the GEANT4 [8] package has been developed. Simulated events are subject to the same reconstruction and selection procedures as the data. MC simulation includes photon jet radiation by initial electrons calculated according to Refs. [9]. Background was estimated using a multihadronic Monte Carlo generator [10] based on experimental data for all measured processes in the energy range up to 2.007 GeV.

The analysis uses about 90 pb^{-1} of an integrated luminosity collected in four scans at 122 energy points in the $E_{c.m.}$=0.9–2.007 GeV range. The scans were performed in 2011, 2012, 2013 and 2017. In the two last scans the beam energy $E_{beam} = E_{c.m.}/2$ has been monitored by using the Back-Scattering-Laser-Light system [11, 12] which determines $E_{c.m.}$ with about 0.06 MeV accuracy at each energy point.

3 Event Selection

Signal identification of $e^+e^- \to 2\pi^0\pi^+\pi^-$ is based on detection of two charged pions and four photons from the decays of two π^0 mesons. The tracks are required to originate from the beam interaction region within 10 cm along the beam axis (Z-coordinate) and within 0.2 cm in the transverse direction and to be in the polar angle range $[0.7 \div \pi - 0.7]$ radians as well as to have ionization losses in DC as shown by lines in Fig. 1 (left).

Four photons with energy larger than 20 MeV and with polar angles in the range $[0.7 \div \pi - 0.7]$ radians are used to create a list of π^0 candidates by requiring that $0.45 < m_{\gamma\gamma} < 0.24$ GeV/c^2. For each pair of oppositely charged tracks and π^0 candidates we perform a kinematic fit with five constraints (5C) of energy-momentum balance and $m_{\gamma_1\gamma_2} = m_{\pi^0}$. The candidates with the minimum value of χ^2_{5C} and $\chi^2_{5C} < 40$ are used in the following analysis. The spectrum of the χ^2_{5C} is shown in Fig. 1 (right). To further suppress background we require
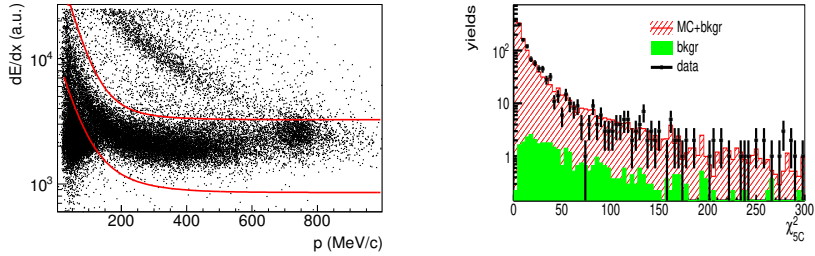
Figure 1. (left) Ionization losses vs. momentum for positive tracks for data at $E_{c.m.} = 1.5$ GeV. The lines show the acceptance for signal pions. (right) The spectrum of χ^2_{5C} for the $e^+e^- \rightarrow 2\pi^0\pi^+\pi^-$ events.

that the reconstructed energy of each photon is greater than 40 MeV and the invariant mass of the third and fourth photons belongs to the range $100 < m_{\gamma_3\gamma_4} < 160$ MeV/c^2. The spectrum of $m_{\gamma_3\gamma_4}$ is shown in Fig. 2 (left) with a sum of signal and background distributions. The signal and background line shapes are obtained from the signal and background simulations.
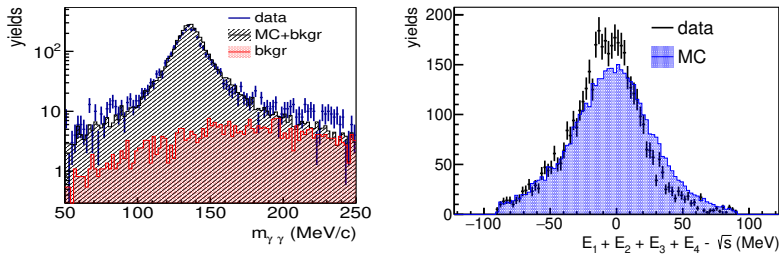

Figure 2. (left) The $\gamma_3\gamma_4$ mass spectrum for $e^+e^- \rightarrow 2\pi^0\pi^+\pi^-$ events at $E_{c.m.} = 1.5$ GeV. (right) The difference of the total reconstructed energy of pions and $\sqrt{s} = E_{c.m.}$ for $e^+e^- \rightarrow 2\pi^+2\pi^-$ events at $E_{c.m.} = 1.5$ GeV.

Identification of events of the $e^+e^- \rightarrow 2\pi^+2\pi^-$ process is based on a search for two positive and two negative tracks with total momentum $|\vec{P_1} + \vec{P_2} + \vec{P_3} + \vec{P_4}|$ less than 90 MeV/c. The requirements on polar angles and dE/dx are the same as for the selection of tracks of the process $e^+e^- \rightarrow 2\pi^0\pi^+\pi^-$, described above. The selected candidates are subject to a kinematic fit (4C) with energy-momentum constraints. The events with $\chi^2_{4C} < 100$ and $\Delta E < 90$ MeV are used for further analysis, where ΔE is the difference of the total reconstructed energy of pions and $E_{c.m.}$ (see Fig. 2(right)).

After all the selections are applied, we are left with 64000 and 72000 candidate events for the $e^+e^- \rightarrow 2\pi^0\pi^+\pi^-$ and $e^+e^- \rightarrow 2\pi^+2\pi^-$ final states, respectively. The amplitude analysis described in the next section treats each event in the data sample as a signal event. The fraction of backgrounds is less than 0.3% according to the multihadronic Monte Carlo generator [10] with normalization to luminosity. The obtained numbers of events normalized to detection efficiency, luminosity and radiative correction allow to obtain the Born cross sections of the processes under study. The cross section of the neutral mode $\sigma(e^+e^- \rightarrow 2\pi^0\pi^+\pi^-)$ is shown in Fig. 3.

4 Amplitude analysis

In order to construct a model of the intermediate structure of the reaction $e^+e^- \to 4\pi$, we perform an amplitude analysis by the minimization of unbined Likelihood function for a particular model

$$
L = -\ln \prod_i^{e^+e^- \to 2\pi^0\pi^+\pi^-} \frac{|\sum_\alpha \mathbf{V}_\alpha A_\alpha^0(\Omega_i)|^2}{\frac{1}{N_{MC}^{gen}} \sum_k^{\text{rec. ph. space MC}} |\sum_\alpha \mathbf{V}_\alpha A_\alpha^0(\Omega_k)|^2}
$$

$$
- \ln \prod_j^{e^+e^- \to 2\pi^+2\pi^-} \frac{|\sum_\alpha \mathbf{V}_\alpha A_\alpha^\pm(\Omega_j)|^2}{\frac{1}{N_{MC}^{gen}} \sum_k^{\text{rec. ph. space MC}} |\sum_\alpha \mathbf{V}_\alpha A_\alpha^\pm(\Omega_k)|^2}, \tag{1}
$$

where i and j runs over all selected events in the $e^+e^- \to 2\pi^0\pi^+\pi^-$ and $e^+e^- \to 2\pi^+2\pi^-$ modes, respectively. The sum α runs over all intermediate states, $\mathbf{V}_\alpha$ - a complex model parameter. The production $\mathbf{V}_\alpha A_\alpha^\pm\big(p_1(\pi^+), p_2(\pi^-), p_3(\pi^+), p_4(\pi^-)\big)$ and $\mathbf{V}_\alpha A_\alpha^0\big(p_1(\pi^0), p_2(\pi^0), p_3(\pi^+), p_4(\pi^-)\big)$ are the specific components α of the total matrix elements at particular points in phase space for the $e^+e^- \to 2\pi^+2\pi^-$ and $e^+e^- \to 2\pi^0\pi^+\pi^-$ channels, respectively. The sum in denominator runs over all MC events, flatly generated in phase space and passed all selection criteria described above. In the model we account for the following contributions (components): $\omega\pi^0$, $a_1^\pm\pi^\mp \to \rho^\pm\pi^\mp\pi^0$, $a_1^\pm\pi^\mp \to \sigma\pi^\pm\pi^\mp$, $\rho^+\rho^-$, $\rho^0\sigma$, $\rho^0 f_0(980)$, $\rho^0 f_2$, $h_1\pi \to \rho^\pm\pi^\mp\pi^0$, $h_1\pi \to \rho^0\pi^0\pi^0$. The channels $\omega\pi^0$, $\rho^+\rho^-$ and $h_1\pi$ contribute only to the process $e^+e^- \to 2\pi^0\pi^+\pi^-$. The parametrization of the different components of the matrix element is the same as used in Ref. [3]. Each specific amplitude satisfies the C invariance: $A_\alpha^0(p_1, p_2, p_3, p_4) = -A_\alpha^0(p_1, p_2, p_4, p_3)$, Bose symmetry: $A_\alpha^0(p_1, p_2, p_3, p_4) = A_\alpha^0(p_2, p_1, p_3, p_4)$ and Gauge invariance: $q^\mu A_\mu(p_1, p_2, p_3, p_4) = 0$, where $q = p_{e^-} + p_{e^+}$ is the sum of the momenta of initial electron and positron. Also in the isospin limit that is assumed in this paper the matrix element for the $e^+e^- \to 2\pi^+2\pi^-$ process can be expressed in terms of the matrix element for the $e^+e^- \to 2\pi^0\pi^+\pi^-$ channel: $A_\alpha^\pm\big(p_1(\pi^+), p_2(\pi^-), p_3(\pi^+), p_4(\pi^-)\big) = A_\alpha^0\big(p_1, p_2, p_3, p_4\big) + A_\alpha^0\big(p_3, p_2, p_1, p_4\big) + A_\alpha^0\big(p_1, p_4, p_3, p_2\big) + A_\alpha^0\big(p_3, p_4, p_1, p_2\big)$. Masses and central values of resonance widths are fixed according to PDG [13].

In Fig. 4 you can see an example of the comparison of the presented model with experimental data for the $e^+e^- \to 2\pi^0\pi^+\pi^-$ process. The peak in the $m_{3\pi}$ spectrum corresponds to the ω-meson, in the $m_{\pi^+\pi^-}$ one - to the ρ^0-meson, in the $m_{\pi^0\pi^0}$ spectrum - to the $f_0(980)$-meson and the peak in $m_{\pi^\pm\pi^0}$ - to the $\rho^\pm$.

Figure 5 demonstrates the comparison of the obtained model and data for the $e^+e^- \to 2\pi^+2\pi^-$ reaction. The left figure is the spectrum of the squared matrix element $|M|^2 = |\sum_\alpha \mathbf{V}_\alpha A_\alpha^\pm(\Omega)|^2$. The only structures related to the production of ρ^0 and $f_0(980)$-mesons are seen in the $\pi^+\pi^-$ mass spectrum. So, the submass projections for the $e^+e^- \to 2\pi^+2\pi^-$ process are less informative than the projections for the $e^+e^- \to 2\pi^0\pi^+\pi^-$ events.

A fraction f_X of an individual component of the matrix element is calculated as

$$
f_X = \frac{\int |\mathbf{V}_X A_X(\Omega)|^2 d\Omega}{\int |\sum_\alpha \mathbf{V}_\alpha A_\alpha(\Omega)|^2 d\Omega}. \tag{2}
$$

The values of f_X multiplied by the cross section $\sigma(e^+e^- \to 2\pi^0\pi^+\pi^-)$ are shown in Fig. 3. Only statistical errors are presented in the figure. In the figure two amplitudes $\rho\sigma$ and $\rho f_0(980)$ are combined into a common one. Independently of the fraction of each amplitude we also vary the phase of the amplitude. In order to avoid the oversaturation of the content, we do not show the values of the phases in this paper.
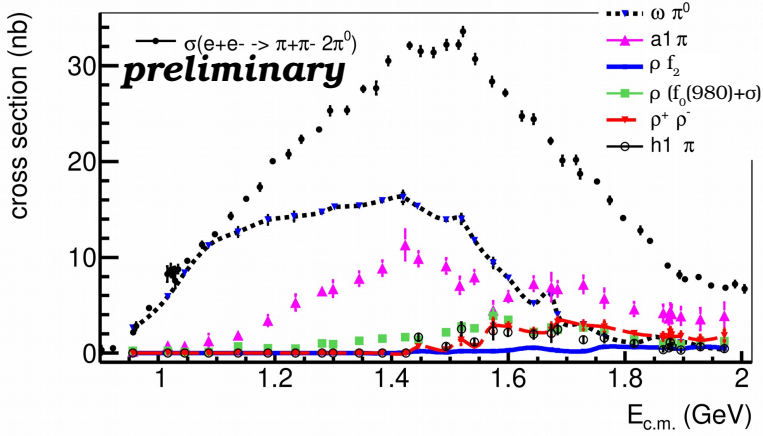
Figure 3. Cross sections calculated for different components of the matrix element. The total cross section of the process $e^+e^- \rightarrow 2\pi^0\pi^+\pi^-$, measured in this analysis (filled circles).
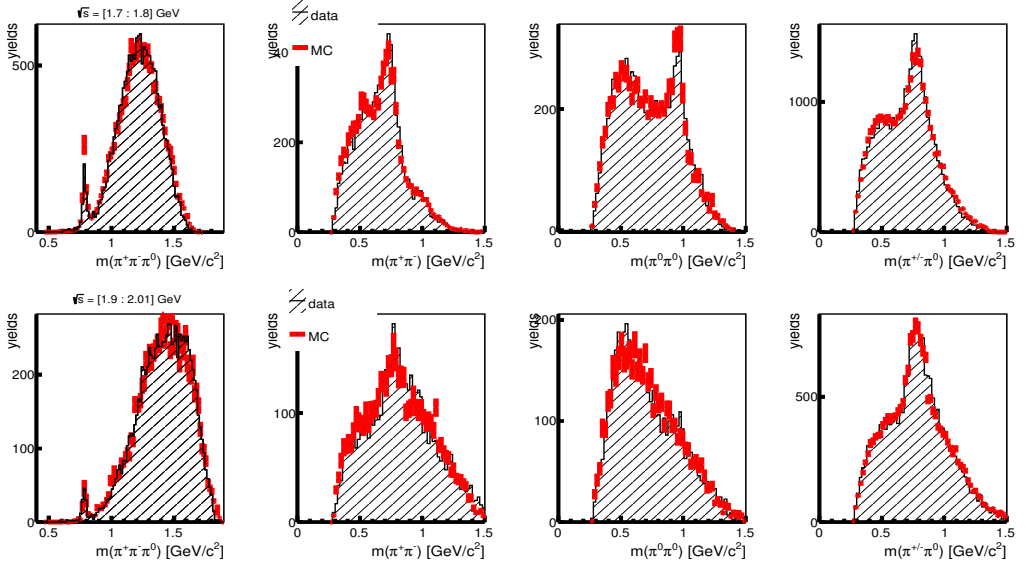

Figure 4. The data-MC comparison of the $\pi^+\pi^-\pi^0$, $\pi^+\pi^-$, $\pi^0\pi^0$ and $\pi^\pm\pi^0$ mass spectra for the process $e^+e^- \rightarrow 2\pi^0\pi^+\pi^-$ in the energy ranges $\sqrt{s} = 1.7 \div 1.8$ GeV (top) and $\sqrt{s} = 1.9 \div 2.01$ GeV (bottom).

5 Systematic and model uncertainty

The preliminary values of the systematic uncertainties for the fractions f_X are estimated as 7% and include three types. First, the uncertainty due to the effect of backgrounds because the analysis is performed with the assumption that all backgrounds have been eliminated. This uncertainty is estimated as a relative difference between results obtained with the loosened and standard selection criteria, which correspond to the cases with different intensities of
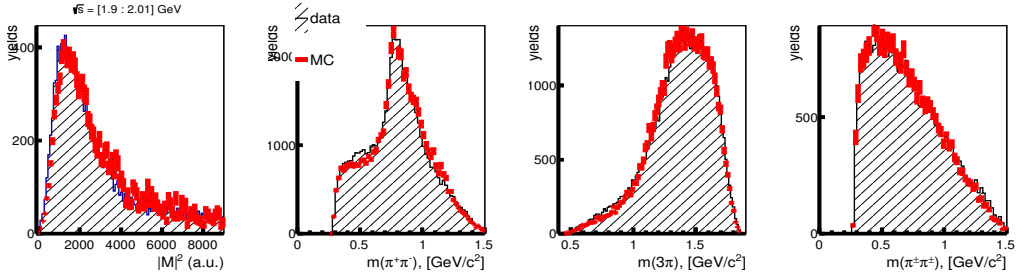
Figure 5. The data-MC comparison of the squared matrix element $|M|^2$ and $\pi^+\pi^-$, $2\pi^\pm\pi^\mp$ and $\pi^\pm\pi^\pm$ mass spectra for the process $e^+e^- \rightarrow 2\pi^+2\pi^-$ for the energy ranges $\sqrt{s} = 1.9 \div 2.01$ GeV.

backgrounds. We lose the standard criteria, described in Sec. 3, $100 < m_{\gamma_3\gamma_4} < 160$ MeV/c^2 to $70 < m_{\gamma_3\gamma_4} < 190$ MeV/c^2 and $\Delta E < 90$ MeV to $\Delta E < 150$ MeV. Second, there is non-perfect simulation of the detector resolution (see, e.g., Fig. 2(right)), that was taken into account by additional smearing of angles and momenta of reconstructed particles in MC simulation. Third, simulation of efficiencies for reconstruction of charged and neutral pions is hardly correct. The most important effect is raised from the data-MC difference of the probability of merging clusters in the calorimeter belonging to photons from π^0-decay. This effect was taken into account by tuning the inefficiency of π^0 reconstruction in MC simulation.

Unlike the systematic uncertainty, there is no direct way to estimate the size of a model one. First, there are other amplitudes ($\pi'(1300)\pi$, $a_2(1320)\pi$ and etc.) that were not tested yet in the analysis. Second, to estimate the model uncertainty we use various modifications of the nominal model and repeat the fit to the data. In particular, we add to the model the phase-space amplitude $A^0\big(p_1(\pi^0), p_2(\pi^0), p_3(\pi^+), p_4(\pi^-)\big) = V_{ph.sp.} \cdot (p_3 - p_4)$ with a free complex parameter $V_{ph.sp.}$. We fix the phases of the less sizable amplitudes ρf_2 and $h_1\pi$ to their average values. We also modify the parametrization of the propagator of the S-wave two-pion system from Flatte to K-matrix formalism. Variations in fit parameters and fractions of contributing channels determined from amplitude analyses with these models are taken as an estimation of the model-related uncertainty, which is about 3%, 15%, 20%, 25%, 40%, 50% and 50% for the $\omega\pi^0$, $a_1\pi$, $\rho(f_0(980) + \sigma)$, $\rho^+\rho^-$, ρf_2 and $h_1\pi$ contributions, respectively.

6 Summary

In conclusion, we have performed a full amplitude analysis of four-body electron-positron annihilation $e^+e^- \rightarrow 4\pi$ that allowed us to determine the relative fractions of various components of the hadronic current of the process. Our preliminary results prove the dominance of the $\omega\pi^0$ and $a_1\pi$ components, however, the contribution of other amplitudes is sizable. A publication with full description of amplitude analysis and the measurement of the cross section is expected soon.

References

[1] J. P. Lees *et al.* (BABAR Collaboration), Phys. Rev. D **376**, 092009 (2017).

[2] J. P. Lees *et al.* (BABAR Collaboration), Phys. Rev. D **85**, 112009 (2012).

[3] R.R. Akhmetshin *et al.* (CMD-2 Collaboration), Physics Letters B **466** 392–402 (1999).

[4] K. W. Edwards *et al.* (CLEO Collaboration), Phys. Rev. D **61**, 072003 (2000).

[5] B. I. Khazin *et al.*, Nucl. Phys. B (Proc. Suppl.) **376**, 181 (2008).

[6] Yu. M. Shatunov *et al.*, in Proceedings of the 7th European Particle Accelerator Conference, Vienna, 2000, p. 439.

[7] V. M. Aulchenko *et al.*, JINST **10**, P10006 (2015).

[8] S. Agostinelli *et al.* (GEANT4 Collaboration), Nucl. Instr. and Meth. A **506**, 250 (2003).

[9] S. Actis *et al.* (Working Group for Radiative Corrections and Monte Carlo Generators at Low Energies), Eur. Phys. J. C **66**, 585 (2010).

[10] H. Czyż *et al.*, arXiv:1312.0454.

[11] E. V. Abakumova *et al.*, Nucl. Instrum. Methods Phys. Res., Sect. A **744**, 35 (2014).

[12] E. V. Abakumova *et. al.*, JINST **10**, T09001 (2015).

[13] M. Tanabashi *et al.* (Particle Data Group), Phys. Rev. D **98**, 030001 (2018).